Subantarctic cyclones identified by 14 tracking methods, and their role for moisture transports into the continent

Grieger, Jens; Leckebusch, Gregor; Raible, Christoph C.; Rudeva, Irina; Simmonds, Ian

DOI:
10.1080/16000870.2018.1454808

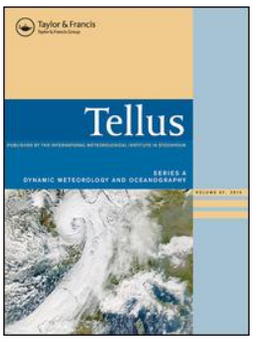

Tellus A: Dynamic Meteorology and Oceanography

ISSN: (Print) 1600-0870 (Online) Journal homepage: http://www.tandfonline.com/loi/zela20

Subantarctic cyclones identified by 14 tracking methods, and their role for moisture transports into the continent

Jens Grieger, Gregor C. Leckebusch, Christoph C. Raible, Irina Rudeva & Ian Simmonds

To cite this article: Jens Grieger, Gregor C. Leckebusch, Christoph C. Raible, Irina Rudeva & Ian Simmonds (2018) Subantarctic cyclones identified by 14 tracking methods, and their role for moisture transports into the continent, Tellus A: Dynamic Meteorology and Oceanography, 70:1, 1454808, DOI: 10.1080/16000870.2018.1454808

To link to this article: https://doi.org/10.1080/16000870.2018.1454808

Published online: 06 Apr 2018.

Tellus SERIES A DYNAMIC METEOROLOGY AND OCEANOGRAPHY
PUBLISHED BY THE INTERNATIONAL METEOROLOGICAL INSTITUTE IN STOCKHOLM

Subantarctic cyclones identified by 14 tracking methods, and their role for moisture transports into the continent

By JENS GRIEGER[1*], GREGOR C. LECKEBUSCH[2], CHRISTOPH C. RAIBLE[3], IRINA RUDEVA[4,5] and IAN SIMMONDS[4], [1]*Institute of Meteorology, Freie Universität Berlin, Berlin, Germany;* [2]*School of Geography, Earth and Environmental Sciences, University of Birmingham, Birmingham, UK;* [3]*Climate and Environmental Physics, and Oeschger Centre for Climate Change Research, University of Bern, Bern, Switzerland;* [4]*School of Earth Sciences, The University of Melbourne, Parkville, Australia;* [5]*P. P. Shirshov Institute of Oceanology, RAS, Moscow, Russia*

(Manuscript received 25 July 2017; in final form 14 March 2018)

ABSTRACT

Extra-tropical cyclones in the subantarctic play a central role in the poleward transport of heat and moisture into Antarctica, with the latter being a key component of the mass balance of the Antarctic ice sheet. As the climate in this region undergoes substantial changes, it is anticipated that the character of these synoptic features will change. There are a number of different methods used to identify and track cyclones, which can potentially lead to different conclusions as to cyclone variability and trends, and mechanisms which drive these features. Given this, it is timely to assess the level of consensus among 14 state-of-the-art cyclone identification and tracking methods. We undertake this comparison with the ERA-Interim data-set for the period 1979–2008 and find large differences in the number of tracks identified by different methods, but the spatial patterns of the system density broadly agree. Links between large-scale modes of variability, such as the Southern Annular Mode (SAM), and subantarctic cyclones as suggested in the literature are confirmed by our analysis. Trends in the number of cyclone tracks show a more diverse picture. Robust trends are identified by almost all methods for austral summer over the region south to 60°S, mainly due to the strong relation to SAM, whereas in austral winter the methods disagree in the statistical significance of the trends. The agreement among the methods is greater when the comparison is confined to the stronger cyclones. This is confirmed by a moisture flux analysis associated with these strong synoptic systems. Our results indicate that multiple cyclone identification and tracking methods should be used to obtain robust conclusions for trends in cyclone characteristics as well as their relation to the large-scale circulation in the subantarctic region.

Keywords: extra-tropical cyclones, IMILAST, cyclone identification, Antarctica, Southern Ocean

1. Introduction

Extra-tropical cyclones are ubiquitous atmospheric features in the mid and high latitudes of the Southern Hemisphere (SH). These owe their existence to a range of complex processes in those regions associated with, e.g. strong baroclinicity (Simmonds and Lim, 2009) and surface fluxes of latent and sensible heat (Uotila et al., 2011). They play a key role in the weather and its extremes over the Southern Ocean (SO) and in the coastal regions of Antarctica (Murphy and Simmonds, 1993). Extra-tropical cyclones also play a fundamental climatological role in balancing the energy budget over the hemisphere. Because of the imbalance between the net radiative inputs into the tropical and higher latitude regions the atmosphere must 'organize' itself to transfer energy (predominantly in the form of latent and sensible heat) from the former to the latter region. In the Northern Hemisphere, stationary waves are responsible for a significant proportion of this transfer (especially in the winter). By contrast, the SH stationary waves contribute very little to the poleward energy transfer at any time of the year, and hence it is left to the transient eddies to carry the required energy (Peixoto and Oort, 1992). The poleward transport of latent energy (or moisture) is of particular relevance to the Antarctic, and thus the mass balance of the Antarctic ice sheet.

Given the influence of these systems it is of importance to monitor and quantify cyclones over the subantarctic and SO

*Corresponding author. e-mail: jens.grieger@met.fu-berlin.de

Citation: Tellus A: 2018, **70**, 1454808, https://doi.org/10.1080/16000870.2018.1454808

regions, especially where the changes in sea ice extent over the past few decades have modified the high latitude baroclinicity (Simmonds, 2015). From the above discussion, one can see that if the net radiative input in the tropical and/or higher latitudes changes, so too does the amount of energy required to be transported poleward. In the SH, this necessity means that a number of characteristics of extra-tropical cyclones must change to balance to the new radiative conditions. Given that cyclones are very complex it is not surprising that quantifying the myriad of cyclone features has proved a challenging task.

For a number of reasons (e.g., data sparsity, hostile environment) synoptic studies in the subantarctic region have been relatively few. In the mid-1990s the international Antarctic First Regional Observing Study of the Troposphere (FROST) project was organized by the Scientific Committee on Antarctic Research (Turner et al., 1996) with a view to, in part, improve regional synoptic analyses and better understand the behavior of high-latitude cyclones. This influential initiative prompted several studies including those of Sinclair (1997), Simmonds and Keay (2000), Simmonds et al. (2003), Simmonds and King (2004), Hoskins and Hodges (2005) and Pezza et al. (2007). These have been valuable in identifying the key climatological features (including the variability and trends) of SH extra-tropical cyclones. However, we point out that each of these studies used a single cyclone identification and tracking method, and hence, the results from a particular study may hold only for the specific scheme used. This general issue has been recognized for many years (Raible et al., 2008), and was one of the reasons for setting up the international Intercomparison of MId LAtitude STorm diagnostics (IMILAST) project to intercompare state-of-the-art algorithms for the identification and tracking of extra-tropical cyclones (Neu et al., 2013). It is within this framework that the present research is conducted and we make use of the subantarctic cyclone sets identified by 14 objective methods which participated in the IMILAST initiative.

SH cyclone activity can be associated with large-scale atmospheric variability such as the Southern Annular Mode (SAM) or El Niño/Southern Oscillation (ENSO) (Pezza et al., 2008, 2012). Local features as the Amundsen Bellingshausen Sea Low (ABSL) influence weather and climate in the environs of the Amundsen Sea by steering cyclones towards West Antarctica (Fogt et al., 2012). The robustness of such links between these large-scale phenomena and cyclone activity is addressed in this paper. In addition to comparing and contrasting the SO cyclone behavior as diagnosed by the different schemes, we also analyze the extent to which diagnosed cyclonic moisture transports to the Antarctic depend on the particular cyclone identification scheme used.

In the following section, the data-set and the methods used are discussed. The statistics of subantarctic cyclones derived from the different schemes are presented in Section 3. This section includes cyclone frequency trends, a cross-correlation analysis between the different algorithms as well as a track-to-track comparison. In addition, the relationship between large-scale circulation and cyclone characteristics is investigated, and how the apparent nature of this relationship may depend on identification method. The analysis also includes a focus on strong cyclones, and an assessment of how much of the meridional moisture flux can be attributed to these systems. Section 4 presents a discussion and Section 5 summary and conclusion of the key findings of the investigation.

2. Data and methods

We base our study of cyclone behavior around Antarctica on 30 years (1979–2008) of ERA-Interim reanalysis (Dee et al., 2011). This data-set is generally acknowledged to be superior to other contemporary reanalyses over our region of interest (e.g., Bracegirdle and Marshall, 2012). The output of 14 state-of-the-art methods for mid-latitude cyclone identification and tracking (Neu et al., 2013) is analyzed for the winter (JJA) and summer (DJF) seasons. The ERA Interim analyses are available every 6 h, and that is the frequency at which the subantarctic cyclones are identified in all but one of the methods (the exception being Method M06 which uses 12-hourly values). Cyclone identification methods can be grouped concerning used input variables. The nature of a cyclone is generally reflected in the mass and wind fields. Therefore, it is dynamically appropriate to identify these systems in terms of either mass (represented by variables such as mean sea level pressure (MSLP) or geopotential height) or vorticity (which represents the rotational component of the wind field). Vorticity can also be computed with the Laplacian of MSLP by means of the quasi-geostrophic assumption. Most methods of this study use mass-representing variables (M08, M12, M14, M15, M16, M20, M22). Three methods use vorticity as calculated from the Laplacian of MSLP (M02, M09, M10), and three methods use vorticity at the 850 hPa pressure level (M07, M18, M21). Additionally there is one hybrid method (M06). References for each of the methods and an overview of the input variables used are given in Table 1. Note that cyclone tracks over high topography, here taken as in excess of 1500 m, are excluded from the analysis as pressure and geopotential height is extrapolated over high orography, which may lead to unphysical values and potential identification of spurious lows.

2.1. *Definition of subsets of cyclone track data*

2.1.1. Temporal and spatial selection. The present work extends the comprehensive analyses already performed by the international IMILAST community, by exploring winter and summer SH cyclones in the subantarctic region. Each cyclone track is 'binned' into a given season if at least one of its time steps falls into the corresponding period. We follow a similar procedure for the spatial allocation of tracks. For example, we require that tracks must be identified at least once south of 60°S

Table 1. Used methods in this paper. Enumeration of the IMILAST members is same as in Neu et al. (2013). Methods which do not provide cyclone central core pressure are printed in italics.

Method	Reference	Variable used
M02	Murray and Simmonds (1991a); Pinto et al. (2005)	MSLP, VORT
M06	Hewson and Titley (2010)	MSLP, VORT, wind, fronts
M07	Flaounas et al. (2014)	Z850 VORT
M08	Trigo (2006)	MSLP
M09	Serreze (1995); Wang et al. (2006)	MSLP, VORT
M10	Murray and Simmonds (1991a); Simmonds et al. (2008)	MSLP, VORT
M12	Zolina and Gulev (2002); Rudeva and Gulev (2007)	MSLP
M14	Kew et al. (2010)	Z850
M15	Blender et al. (1997); Raible et al. (2008)	MSLP
M16	Lionello et al. (2002)	MSLP
M18	Sinclair (1994, 1997)	Z850 VORT
M20	Wernli and Schwierz (2006)	MSLP
M21	Inatsu (2009)	Z850 VORT
M22	Bardin and Polonsky (2005); Akperov et al. (2007)	MSLP

to be considered in our analysis (named *S60* in the following). Because the behavior of cyclones considerably differs with longitude it is of value to also consider these cyclones over three key sectors lying to the south of 60°S, namely East Antarctica (*EA*) (0°–180°), the Amundsen-Bellingshausen Sea (*ABS*) (180°–60°W), and the Weddell Sea (*WED*) (60°W–0°) (Fig. 1). As above, a track is attributed to one of these longitudinal sectors if it spends at least one synoptic time in it. Hence, it is possible for a track to be attributed to more than one sector.

2.1.2. Definition of strong cyclones. There are numerous ways to physically define the strength (or intensity) of a cyclone. Considering cyclones as low pressure systems, the minimum cyclone core pressure is often used as measure for strength (e.g. Lambert and Fyfe, 2006). Taking also the background and/or climatological field of MSLP into account, the strength can be defined in terms of 'relative' central pressure (e.g., Simmonds and Wu, 1993) or pressure gradient (e.g. Blender et al., 1997; Wernli and Schwierz, 2006). Conversely, one can use the vorticity to define cyclone strength (Hoskins and Hodges, 2005). For quasi-geostrophic conditions, vorticity is proportional to the Laplacian of MSLP, which is also used to define the intensity of cyclones (Murray and Simmonds, 1991a).

One can define strong cyclones in terms of absolute thresholds or percentile thresholds of intensity, e.g. the 95th percentile of the Laplacian of MSLP (Leckebusch and Ulbrich 2004; Leckebusch et al., 2006, 2008; Grieger et al., 2014). In this study we follow the approach of Ulbrich et al. (2013), and take as 'strong cyclones' the most intense 500 winter cyclone tracks for the 30-year data-set (these representing about 5.5% of all identified winter tracks). For simplicity, the minimum MSLP is used as intensity measure since 10 out of 14 methods provide this quantity (Table 1). Note that the intensity thresholds for the different methods can differ (Rudeva et al., 2014) and thus are adjusted to ensure that the same number of tracks are in the strong cyclone data-set.

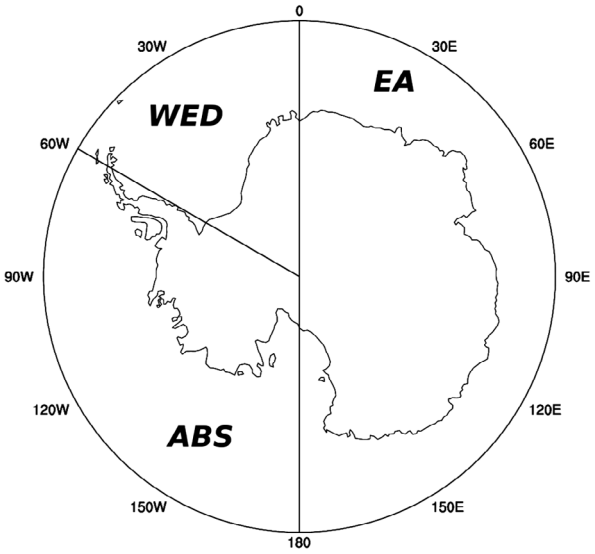

Fig. 1. The Antarctic continent and the surrounding SO south of 60°S, referred to as *S60* in this study. Also shown are the three sectors, i.e. East Antarctica (0°–180°, *EA*), Amundsen-Bellingshausen Sea (180–60°W, *ABS*), and Weddell Sea (60°W–0°, *WED*), considered here.

2.2. *Track-to-track comparison*

An important aspect of our investigation is to quantify the similarity of cyclone tracks obtained from the different methods. A comparison of individual cyclone tracks identified by the different methods is performed here following the approach of Blender and Schubert (2000). Their track-to-track comparison uses a spatio-temporal metric which quantifies the deviation of the trajectories. The number of 'agreeing trajectories' (based on this metric) is considered in relation to the total number of trajectories of that method which identifies less cyclones resulting in the so-called matching rate. Further details are given in Blender and Schubert (2000), Raible et al. (2008) and Neu et al. (2013).

2.3. *Large-scale circulation indices*

All indices are calculated from 6-hourly ERA Interim MSLP for the seasons (as opposed to an average of three monthly in-

dices). SAM is calculated from the zonal mean difference between 40°S and 65°S as suggested by Gong and Wang (1999). Meneghini et al. (2007) found a closer relationship between Australian precipitation and large-scale activity using a regional SAM index. Following this idea, a 'Pacific SAM' (SAMP) is calculated to investigate the link of this driver on cyclone activity in the region of West-Antarctica and the Antarctic Peninsula where strongest Antarctic climate change occurred during the twentieth century (Turner et al., 2009). SAMP is calculated similar as SAM but only in the Pacific and ABS sectors, taken here as 180°–60°W.

The ABSL is a quasi-stationary low pressure system located at the Amundsen-Bellingshausen Sea sector which largely affects weather and climate of West-Antarctica (Turner et al., 2013; Raphael et al., 2016). While Fogt et al. (2012) identified the minimum SLP in the Amundsen-Bellingshausen Seas to quantify the strength of the ABSL, Hosking et al. (2013) suggested to use an index where the background pressure fields are subtracted to decorrelate the ABSL index from SAM. In this study, the ABSL index is calculated to reflect the meridional pressure gradient anomaly in the ABS region. Therefore, the index is similarly defined as SAMP but slightly shifted southward where the ABSL generally can be identified. The ABSL index is calculated from the MSLP difference between 45°S and 75°S over the ABS sector (180°–60°W).

2.4. *Meridional moisture flux analysis*

Our analysis investigates the role that cyclones, and particularly strong ones, play in transporting moisture to the Antarctic. To quantify this, we consider the vertically integrated meridional moisture flux per unit longitudinal distance

$$Q = \frac{1}{g}\int_{p_0}^{p_{sfc}} q(p)v(p)\mathrm{d}p \tag{1}$$

(Simmonds et al., 1999a) where g is acceleration of gravity, q is specific humidity and v is the meridional wind component. The integration is from the surface pressure p_{sfc} to $p_0 = 200$ hPa using 6-hourly data on 23 pressure levels. To assign the moisture flux to extra-tropical cyclones, which can be attributed to atmospheric transient waves, for each grid point a temporal Reynolds decomposition of the meridional moisture flux has been performed. Hence, the average flux can be written

$$\bar{Q} = \overline{qv} = \bar{q}\bar{v} + \overline{q'v'} \tag{2}$$

where the overbar denotes the time average and the prime the instantaneous temporal deviation from that average. The first part is the transport due to time mean meridional motion and the latter is the component of transient eddies (TE). In the SH extra-tropics, the most important part of meridional transport is due to transient flux perturbations (Peixoto and Oort, 1992). Moisture flux as well as the decomposition of equation 2 is calculated separately for each of the 30 years for JJA. Moisture flux during this season is highly relevant for humidity transport into Antarctica, since net continental precipitation shows its maximum during this part of the year (e.g. Bromwich et al., 1995; Cullather et al., 1998).

In the following, the part of the meridional moisture flux which can be assigned to strong cyclones (these being defined in Section 2.1.2) is determined. To do this the TE component of Q is evaluated by means of a composite study. All days are taken into account, where each of the 500 strong cyclone tracks shows its maximum intensity (minimum core pressure). For these days, the fields of transient moisture flux are averaged over a longitudinal sector of 60° centered on the cyclone center. This composite of 'extreme' transient moisture flux is then subtracted by the climatological mean (30 yr) transient moisture flux to calculate an anomaly of strong flux. This calculation is done for each tracking method separately. This method follows Fogt et al. (2012) who analyzed the influence of strong cyclones within the ABS region. For an easier interpretation of anomaly fields, poleward (towards the south pole) transports are defined to be positive.

3. Results

3.1. *Cyclone track frequencies and intensities*

Consistent with hemispheric results from previous studies (e.g. Neu et al., 2013), the numbers of identified cyclones in the subantarctic region show large differences between the different tracking methods. Figure 2 shows time series of the number of cyclone tracks identified by each method between 1979 and 2008 in our four regions and two seasons. Though the number of tracks can vary by a factor of four depending on the method, the time series demonstrate consistent behavior of the seasonal number of tracks for all methods and regions. The largest number of tracks is detected by M02, M06 and M18 (up to 350 tracks in DJF and 500 in JJA), while M14 and M21 identify only 130–150 and 180–220 tracks in DJF and JJA, respectively. For the reasons discussed above, it is not surprising that the methods which identify the most tracks are vorticity-based (M02, M18). However, it should be pointed out that the method which detects the lowest number of tracks, i.e. M21 is also vorticity-based. Hence, it may not be possible in general to directly relate the number of systems identified to the specific input variable used. As remarked above, the time series exhibit strongly coherent behavior, particularly during the years of large anomalies, e.g. in 1982 and 2000.

In summer, the spread between the various methods is less pronounced than in winter. At first sight, this is counterintuitive, since the climatological mean of cyclones generally is of lower intensity in summer and results of different tracking algorithms are more similar for intense cyclones (Neu et al., 2013; Ulbrich

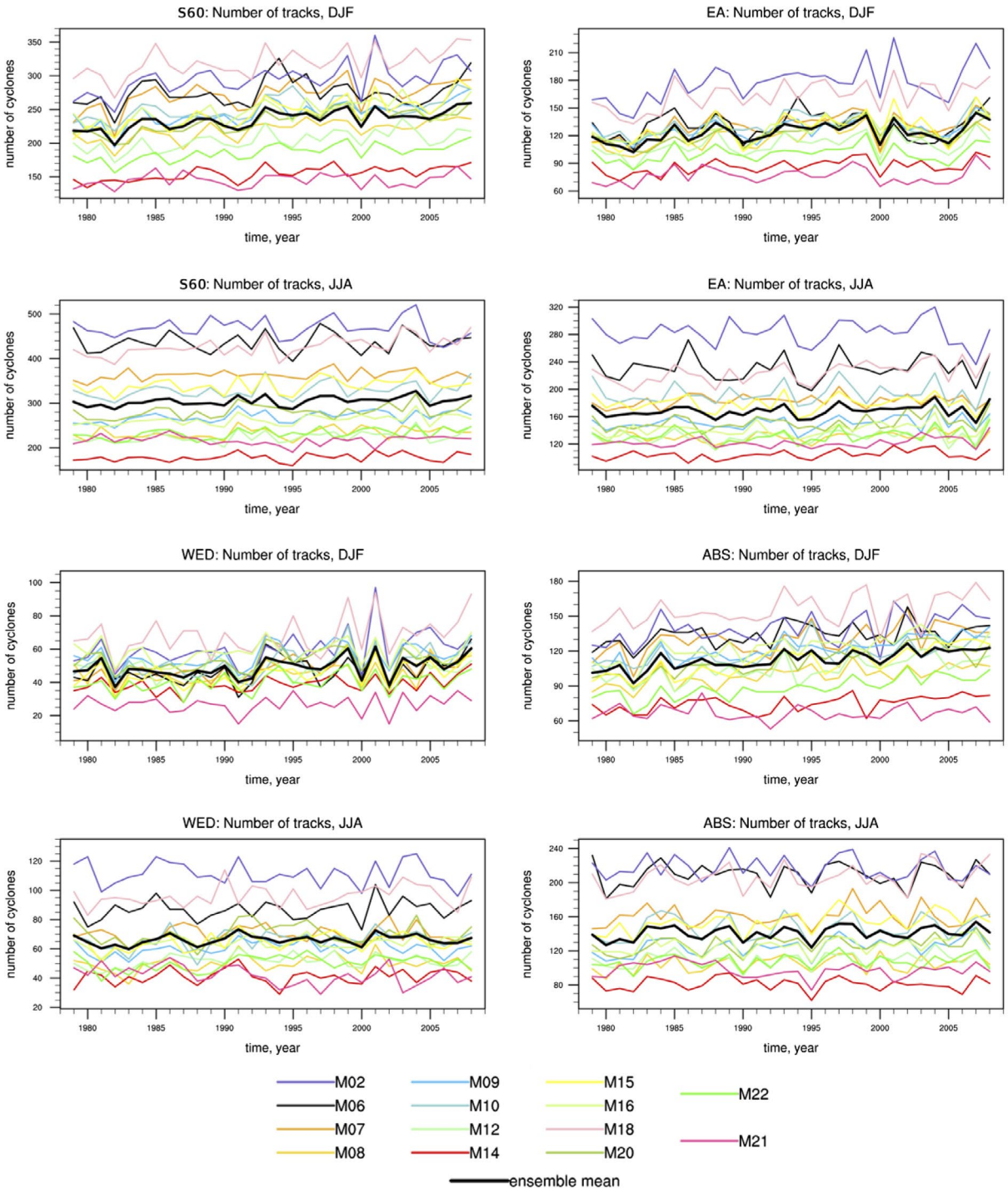

Fig. 2. Time series of number of identified cyclone tracks in the regions *S60*, *EA*, *WED*, *ABS* for austral winter and summer.

et al., 2013). This behavior for summer and winter is observed in all geographical sectors.

For a better understanding of the results concerning the identified number of cyclone tracks by different methods, the cyclone track frequency for both seasons is shown as a function of minimum core pressure of the corresponding track in *S60* (Fig. 3). This analysis is done for all those tracking methods which provide cyclone core pressure (Table 1). Figure 3 shows the density distribution of minimum pressure for each tracking method. Note, that the integral of each curve gives the absolute

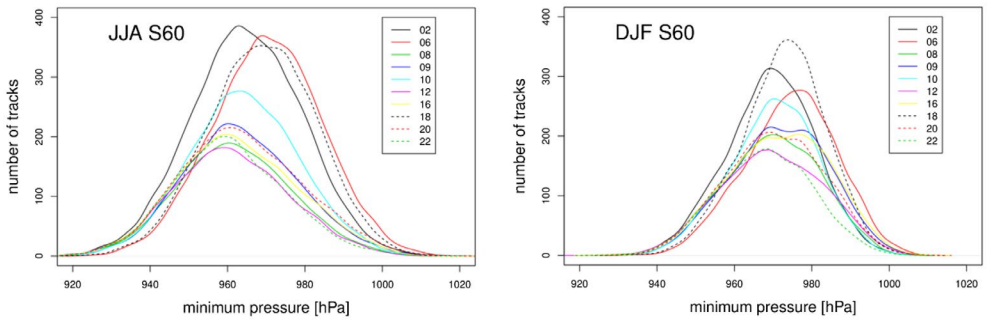

Fig. 3. Density distribution of minimum pressure for each cyclone track in *S60* multiplied by the number of identified tracks for each method identified per season.

number of tracks for each method and season. As expected, core pressures are generally lower for winter. Here, the largest differences between the methods occur for strengths around the peak and for less intense ones. As revealed in previous studies (Neu et al., 2013; Rudeva et al., 2014), there is considerable agreement among the methods in terms of the identification of intense cyclones, e.g., systems with central pressure lower than 950 hPa in winter and 965 hPa in summer.

Note that the methods tend to group themselves in terms of diagnosing similar behavior (e.g. Methods M08, 09, 12, 16, 20, and 22). These examples include only one method which is vorticity based, i.e. M09 while the others use MSLP or geopotential height. The methods which identify most tracks are vorticity based or hybrid methods (M02, M06, M10, M18). Methods 06 and 18 have pressure distributions which are shifted towards higher pressure values and, hence, less intense cyclones. The peak of the distribution is about 970 hPa, whereas all other methods have common peaks around 960 hPa. Methods 02 and 10 use the same tracking algorithm, although the latter applies spatial smoothing before the identification. This explains why M02 shows most cyclone tracks and also identifies cyclones with lowest pressure values.

Distributions of minimum pressure for each cyclone track are generally more similar in summer. The conclusion here is that the generally broader range of extra-tropical cyclone intensity distributions in winter leads to stronger differences between the various methods. Indeed, the frequency distributions associated with the numerous methods differ most for shallow cyclones and agree best for intense ones.

3.2. *Spatial patterns of system density*

Further insight into the analysis of cyclone frequencies represented by the different methods can be obtained by examining the spatial distribution of cyclone system density. The system density is the average number of cyclone counts per synoptic time in a $10^3 \times (°\text{lat})^2$ area, and is calculated at each point of a 2.5° grid using a weighting function that decreases monotonically and is zero for separations greater than 2.5° (see Murray and Simmonds, 1991b).

Figures 4 and 5 show the system density for each method for JJA and DJF, respectively. (Note that no cyclone tracks are identified over Antarctica for the reasons discussed earlier.) In general, both Figures show the different absolute numbers of cyclones identified by the different methods. Note that the system density presented here in Figs. 4 and 5 is not directly comparable to the number of tracks shown in Table 2, because each track consists of a different number of cyclone counts (or track duration). The patterns of system density, especially local maxima, are comparable between the methods (Figs. 4 and 5). Best agreement is found for the local maxima off the coast of Dronning Maud Land at 30°E, near Wilkes Land at 120°E, and over, and to the north of, the Ross Sea. These maxima are associated with climatological MSLP minima in those regions (Schwerdtfeger, 1984) and are more pronounced for winter (Fig. 4). Some methods identify additional local maxima of the system density in the regions of Ronne and Ross ice shelves. Over these domains, the most pronounced differences occur between the methods. Six methods show their absolute maximum system density over at least one of the huge ice shelf regions (M02, M07, M14, M16, M20, and M21), whereas the others do not show pronounced system densities in these regions. M02, M07, and M21 are vorticity-based, M14, M16, and M20 are using geopotential height and MSLP, respectively. M02 and M15 find another local maximum at the Antarctic Peninsula, which is the absolute maximum for M15. M07 is the only method to show an extraordinary pronounced maximum at the Amery Ice Shelf. Most of these deviations can be traced back to topographic features and the sensitivity of the methods to detect local minima associated to those.

A similar picture can be drawn for summer (Fig. 5). Additionally, to the local maxima, which have been identified for winter (Fig. 4), highly pronounced system density maximum over the ABS are found in all methods. This is possibly due to the annual cycle of the ABSL, which is shifted toward the Antarctic Peninsula in summer (Fogt et al., 2012).

To explore whether the agreement between the methods changes for strong cyclones (as defined in Section 2.1.2) the system density is also calculated for those methods which pro-

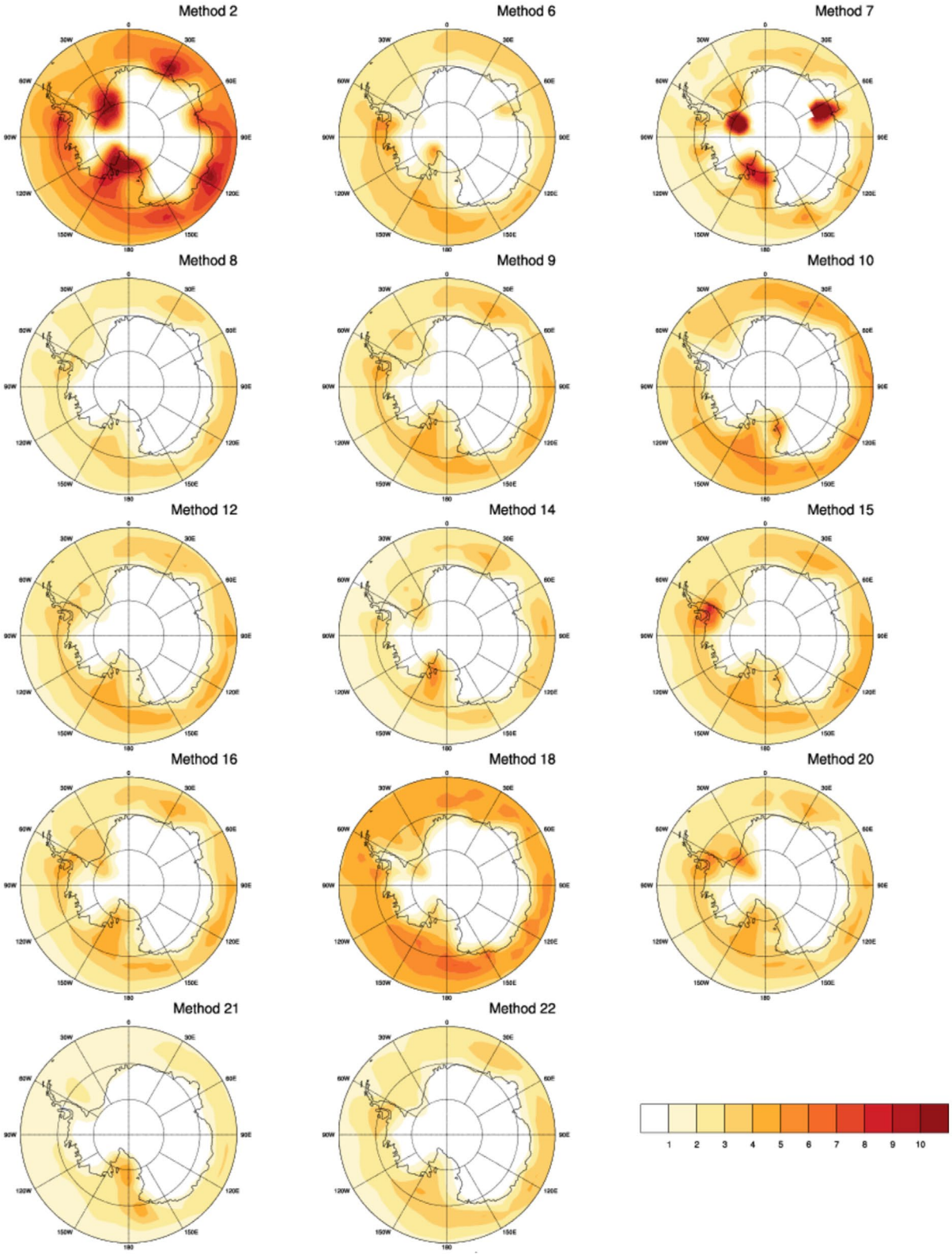

Fig. 4. System density for winter (JJA) [cyclones per 10^3(lat)^2 area per analysis].

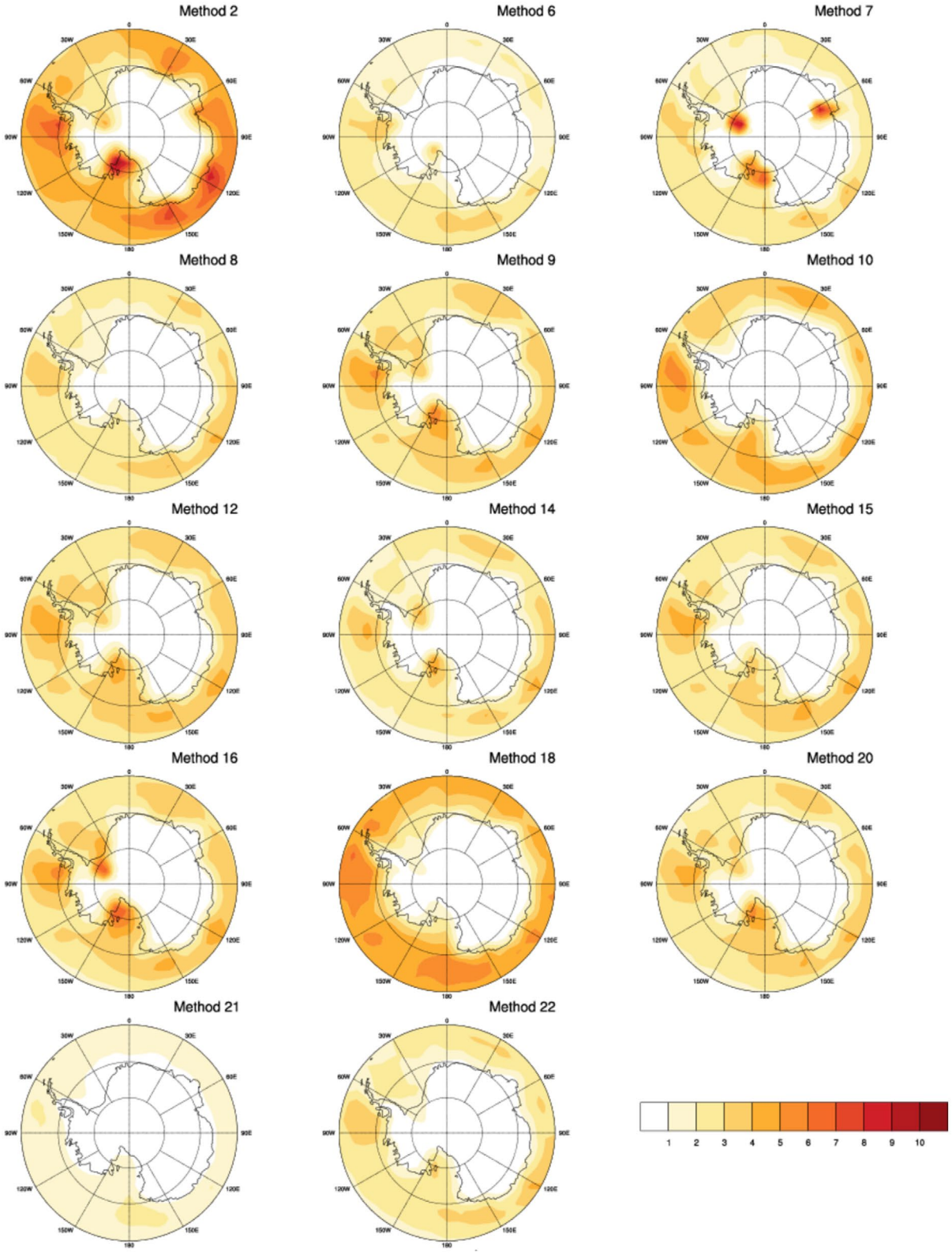

Fig. 5. As Fig. 3 but for summer (DJF) [cyclones per 10^3(lat)^2 area per analysis].

Table 2. Number of *S60* cyclones for winter (JJA, first column) and summer (DJF, first row) detected by each method, and track agreement between methods for winter (lower left triangular matrix) and summer (top-right triangular matrix). Values denote a nominal percentage agreement (relative to the lower number of tracks produced by the two methods) when both methods detect a track at a similar place and time. Values ≥50% are shaded (blue for winter, red for summer), with medium shading for ≥60%, and dark shading for ≥70%.

Method	JJA	M02	M06	M07	M08	M09	M10	M12	M14	M15	M16	M18	M20	M21	M22
DJF	x100	88	82	82	66	73	75	61	46	73	73	96	70	43	56
M02	140	100	50	55	63	62	62	66	70	63	59	52	60	71	69
M06	131	50	100	52	60	56	56	57	63	60	52	52	57	72	65
M07	109	57	55	100	64	59	58	60	68	63	57	54	58	69	60
M08	70	70	70	68	100	73	64	66	72	71	68	58	68	72	78
M09	81	68	65	63	75	100	62	77	78	66	78	52	77	71	86
M10	98	64	60	54	71	67	100	62	67	61	57	61	59	72	71
M12	67	72	67	64	67	78	70	100	71	65	74	57	68	62	71
M14	53	74	70	72	70	74	69	67	100	71	77	64	74	56	74
M15	102	60	60	58	80	76	59	74	75	100	61	59	66	78	75
M16	79	68	64	62	70	77	63	74	74	71	100	49	71	68	81
M18	128	48	49	53	67	61	59	66	68	57	59	100	54	72	62
M20	85	63	60	59	69	71	58	71	71	68	68	57	100	68	79
M21	65	70	69	71	61	64	65	57	63	72	61	68	62	100	67
M22	70	71	70	68	72	83	71	72	72	79	77	66	73	60	100

vide central pressure as cyclone intensity (Table 1). Figure 6 shows the system density of strong cyclones per winter. All methods identify four local maxima, these being located in the ABS sector, one on the Prime meridian, and at 30°E, and 90°E. Thus, we can conclude that strong cyclones are represented by various methods in a more consistent way than including all cyclones in the analysis.

3.3. *Trends in cyclone characteristics*

The atmospheric circulation in the SH has displayed significant changes in recent decades. One of the methods used here has demonstrated significant increases in the number of cyclones in the 50–70°S band (Rudeva and Simmonds, 2015). A significant positive trend of SAM is apparent over the observational period (Hartmann et al., 2013). Fyfe (2003) indicated SH extra-tropical cyclones as 'harbingers of climate change' since changes in their characteristics can be consistently found in the 20th century in the high southern latitudes. In the following, the robustness of the latter statement is analyzed with respect to the identification method used. For such a trend analysis, it is important to use several cyclone tracking and detection methods as trends can be dependent on the method as illustrated by the results of Raible et al. (2008) for the North Atlantic.

Trends of the identified number of cyclone tracks are most significant in summer, particularly for *S60* and *ABS* (Fig. 7). For *S60* all but two methods (M06, M21) identify trends which are significant at the 1% level. The number of tracks increases by 8–19 tracks per season per decade. In winter, seven out of 14 methods show significant positive trends (5% level), but in the other seven methods trends are not significant at the 5% level. In *ABS* and *EA* trends are found to be significant at the 1% level for 12 and 8 schemes, respectively, in DJF. In *WED*, trends are generally less significant. Nevertheless, 9 methods show positive trends in summer which are significant at the 5% level.

It is difficult to classify the methods with respect to their trend behavior for different regions and seasons. During summer, the trend of SAM is a possible indicator of a corresponding cyclone track trend which is robust for different methods. The picture is more diverse for winter. For *S60* M09, M16, and M18 show a significant trend (1% significance level), which is probably due to *EA* for M18 and due to *ABS* for M09. M15 has also a significant (1% level) trend at *ABS*. M09, M15, and M20 show a local maximum of identified tracks over the Antarctic Peninsula. The variability of this feature potentially can influence the trend in the *ABS* region.

3.4. *Cross correlation and track-to-track comparison*

The next component of our intercomparison is a cross correlation analysis of the time series of cyclone frequencies generated by our 14 methods. As discussed in the previous section, the trends in the time series have a considerable degree of similarity and hence, as one might have expected, the correlations are significant for the majority of pairings of methods in regions where trends were found. To highlight the consistency of the interannual variations rather than that of the trends, cross correlation analyses was based on the detrended time series.

Region *EA* shows the best agreement between the methods in both seasons, when in summer all of the 91 possible pairings are statistically significant (5% level), while in winter this is somewhat lower at 79 pairings (Fig. 8). We point out that these numbers are similar for the non-detrended case. Note that the trends over the *EA* region were not as marked as elsewhere. Interestingly, unlike the other regions, in *ABS* the correlation between the detrended time series is higher in winter than in summer. Here, 83 out of 91 pairings show correlation coefficients which are statistically significant at the 5% level with typical r values being between 0.5 and 0.6. The lowest agreement is seen for JJA in *WED*.

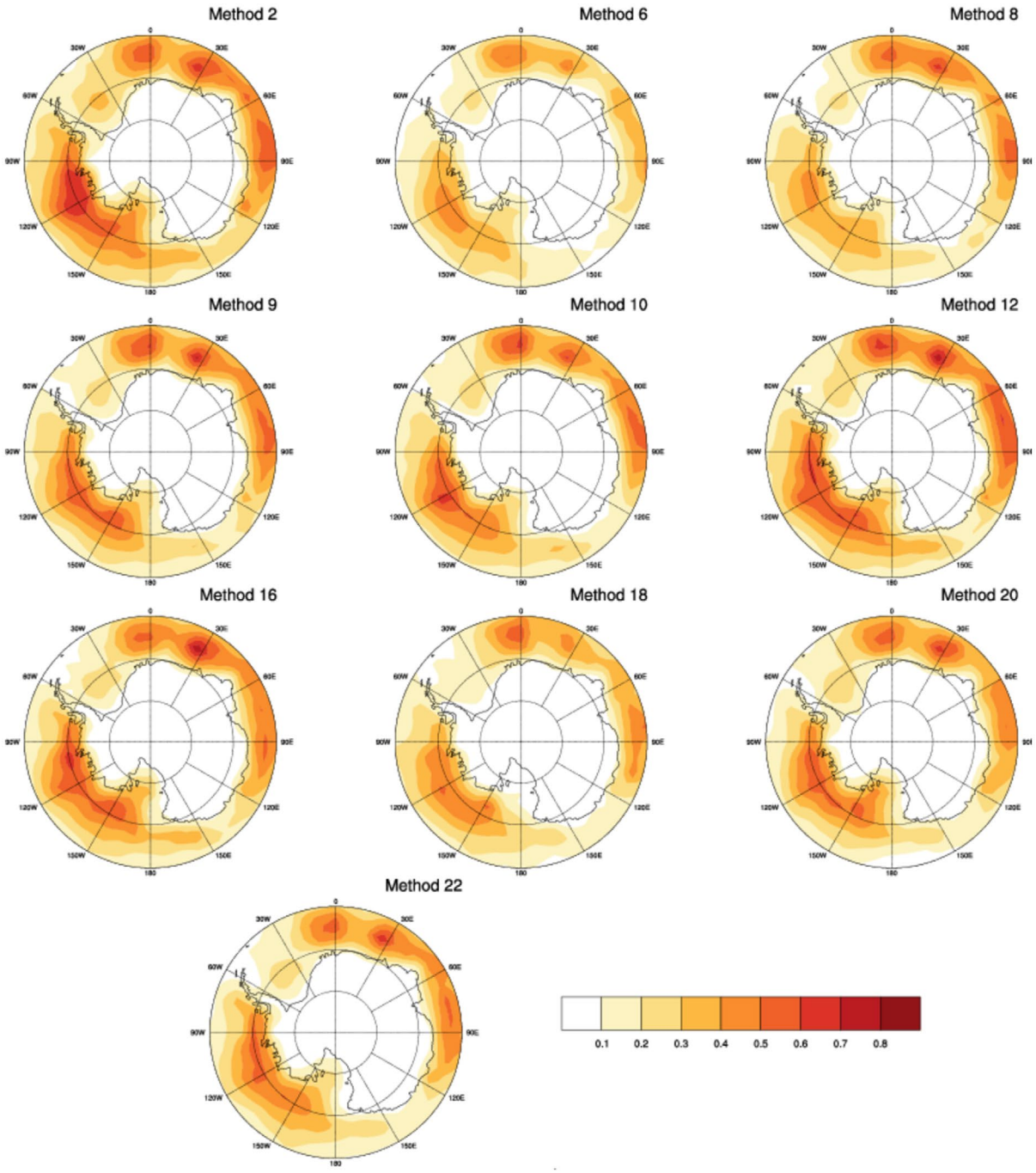

Fig. 6. As Fig. 3 but for strong cyclones for winter (JJA) [cyclones per 10^3(lat)^2 area per analysis].

Table 2 summarizes the results of the track-to-track comparison for *S60* following the approach described in Section 2.2. The matching rate between the different cyclone identification and tracking methods varies across the regions by between 50 and 80% and is consistent with earlier findings for the entire SH (Neu et al., 2013). The matching rates are higher in winter than in summer, and also higher when one of the methods identifies distinctly fewer trajectories. Both results are expected as winter cyclones are deeper and therefore easier to identify. Furthermore, methods showing fewer cyclones tend to find the strong ones which are easier to detect for all methods. We mention that M07 shows somewhat lower matching rates. This method identifies exceptionally high numbers of cyclone tracks over the Ronne, Ross, and Amery Ice Shelves (Figs. 2, 4, and 5)

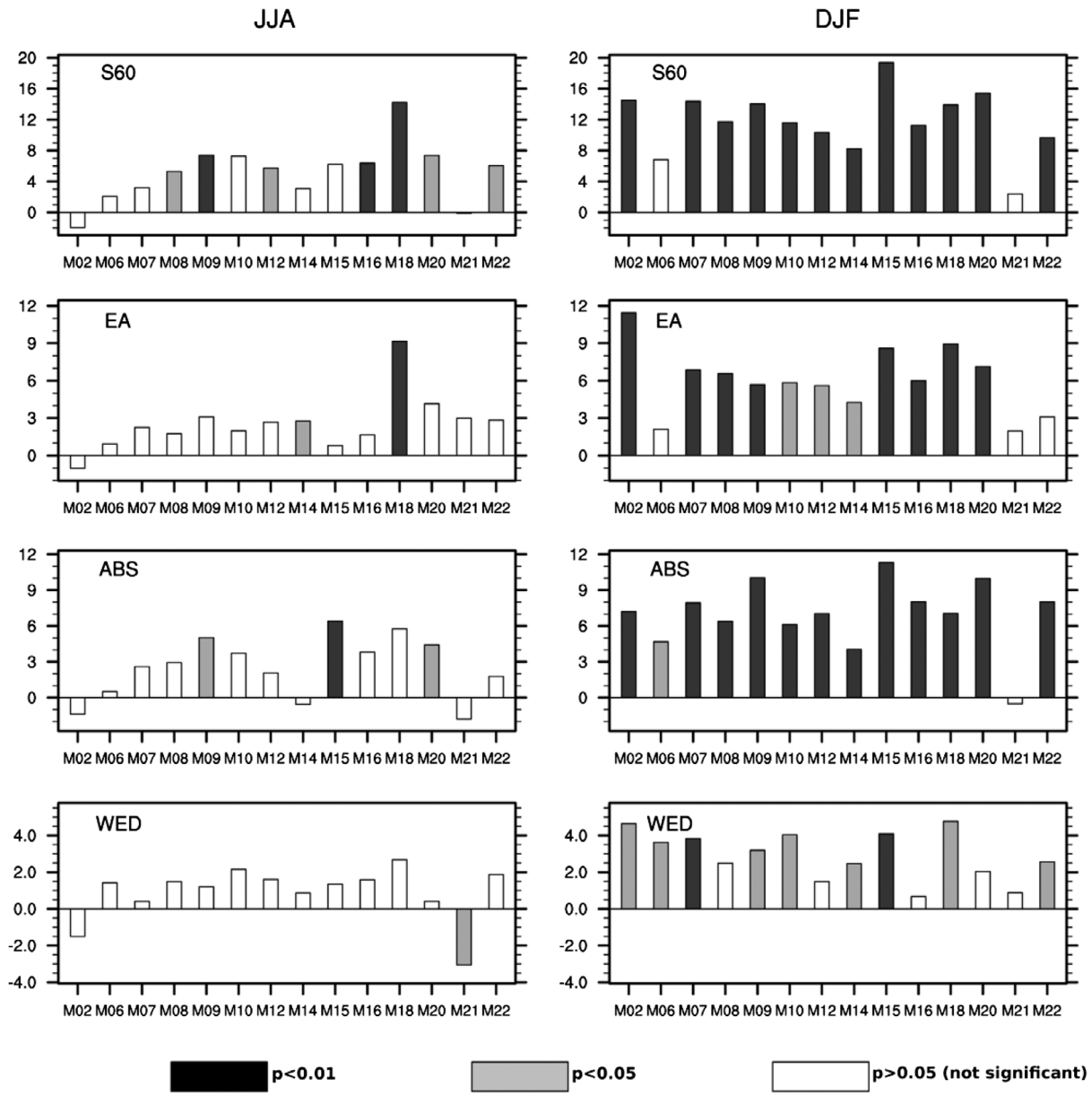

Fig. 7. Decadal trends in the number of cyclone tracks for the regions *S60, EA, WED, ABS,* for (left) winter and (right) summer. The trends are calculated over the period 1979–2008.

which probably explains the low rate. M07 seems to be too sensitive in those regions of steep topography and local wind effects. M18 also shows lower matching rates in comparison with other methods. Especially in summer this method identifies the highest number of cyclones and may include too many weak vorticity maxima, which might increase the risk to erroneously attributing cyclone centers to a given trajectory.

The comparison between the different regions shows that the matching rates differ only slightly (not shown). Thus, the track-to-track comparison shows that the methods are insensitive to the region applied in the SH.

3.5. Relationship between cyclone frequencies and large-scale modes of variability

The SAM is known to be the main mode of atmospheric variability in the high latitudes of the SH, and it is of considerable interest to quantify its relationship with subantarctic cyclones and determine whether the nature of that relationship is robust and applicable across all the methods considered. Our results show that in *S60* and *EA* the DJF number of tracks is highly correlated with the SAM for the majority of methods, but for the other two areas the correlation is often not significant at the 5% level

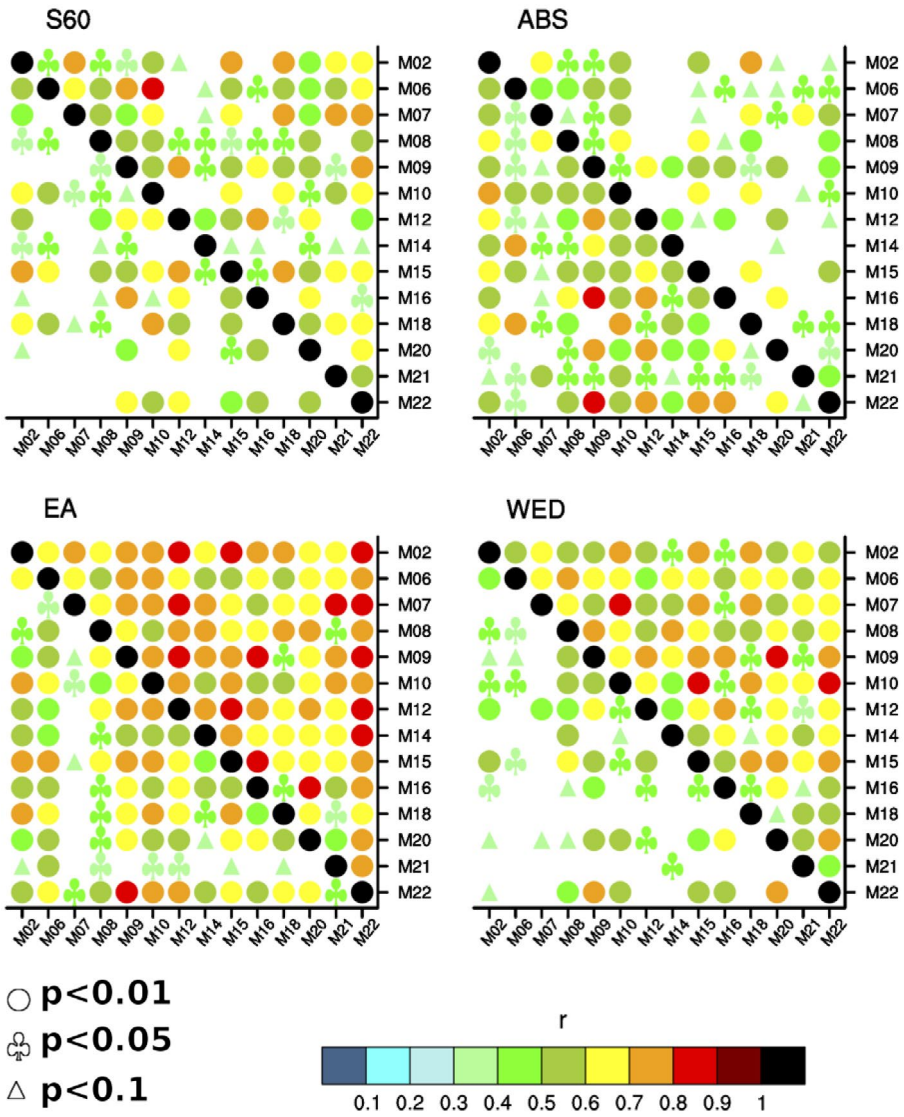

Fig. 8. Cross correlation of detrended time series of the number of cyclone tracks for the regions *S60, EA, WED, ABS* for (upper right triangle) summer and (lower left triangle) winter. Symbols denote significance of the correlation. Non-significant values are not shown.

(Fig. 9). Interestingly, in JJA some methods (M02, M06, M10, M15, M18) demonstrate robust links between the number of tracks in three or even in all four regions, while other methods (M09, M16, M20, M21, M22) show that the correlation is not statistically significant at the 5% level in any region. Regarding the methods which show the robust link to SAM, M02, M10, and M18 are vorticity-based and M06 is a hybrid one, whereas M15 uses geopotential height as input variable.

Since SAMP is defined in the same way as SAM but for the Pacific sector of the SO, cyclone results are expected to be sensitive to it in the *ABS* region. The SAMP index is, indeed, closely related to cyclone activity in *ABS* during the cold months (with only two methods not showing statistically significant correlations at the 5% level, i.e. M20, and M22), however, in summer most schemes do not show statistically significant correlations with this index in this region. Here, the relation with *S60* is more pronounced.

The ABSL index shows highly significant correlations with the DJF number of tracks for all four regions in four methods (M02, M07, M10, and M18) and three regions (excluding *ABS*) in other four methods (M06, M15, M21, M22). For winter, the ABSL index shows significant correlations in M02, M10, and M18 (for all but *WED* regions), while for five other methods (M06, M07, M08, M14, M21) the relationship seems mainly confined to the *ABS* region. The ABSL index seems to show more pronounced correlations with the vorticity-based methods (M02, M07, M10, M18). The strength of ABSL associations with cyclones around the entire Antarctic continent in summer

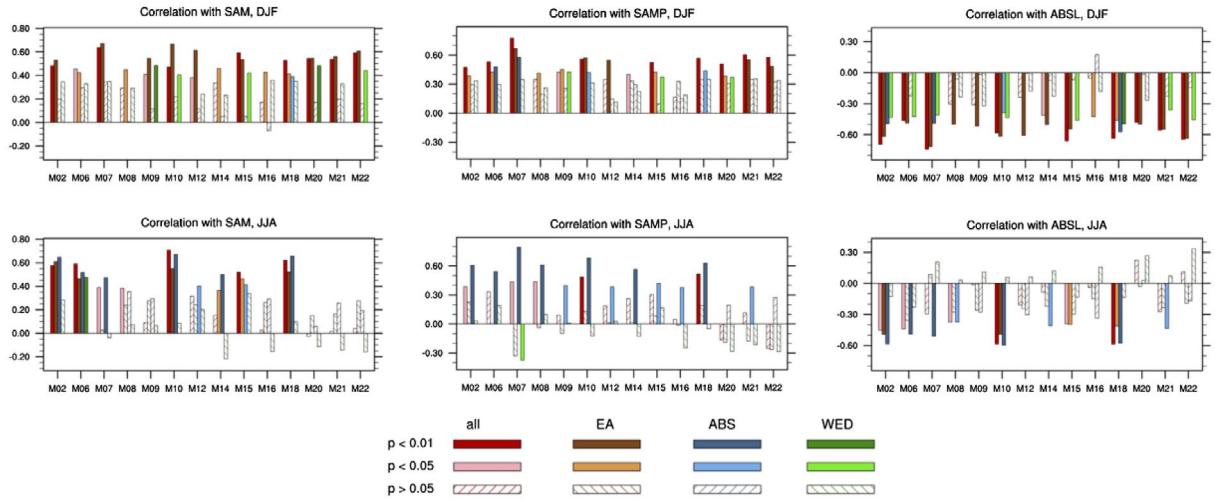

Fig. 9. Correlation between the number of tracks and the index of SAM, SAMP, ABSL for (upper) summer and (lower) winter.

is perhaps surprising (one could have expected a closer connection with (regional) cyclone frequency in *ABS*). Hosking et al. (2013) discussed the strong association between the strength of the ABSL and the SAM due to background pressure field given by variability of the annular mode. This effect potentially leads to the high correlation of ABSL and cyclone frequency in almost all regions. Another perspective on this apparent conundrum is that summer subantarctic cyclones are quite long-lived, with about one-third of tracks (in M10) lasting more than 5 days (Table 1 in Simmonds (2000)) and cyclones can travel significant distances in that time. The ABSL is known to be a 'graveyard' for cyclones (Simmonds et al., 2003) and hence the longevity of the tracks means there is a significant cyclone 'catchment area' for the ABSL which can extend upstream across the Pacific and into the Indian Ocean. Hence, one can understand how cyclones in remote sectors can influence the ABSL.

3.6. *Attribution of moisture flux to strong cyclones*

High latitude cyclones are intimately involved with the meridional moisture flux and thus influencing the mass balance of Antarctica. In the following, we investigate the relation between strong cyclones and the moisture flux (defined in Section 2.4) and assess the extent to which the relation is sensitive to the cyclone detection and tracking method used.

Figure 10 shows the TE component anomaly of the moisture flux due to strong cyclone activity for the 10-method mean as well as the respective deviation from that mean for each method. The method mean (box in Fig. 10) presents the moisture flux anomaly related with strong cyclones (shading) with respect to the climatological mean moisture transport (isolines). As expected, strong cyclone moisture flux anomalies of the method mean are mainly positive, i.e. these systems are responsible for moisture transport exceeding mean flux. The most pronounced region is at Prime meridian, whereas positive anomalies are further found around East Antarctica. The regions north of the Amundsen-Bellingshausen Seas show two local maxima between 120°W and 150°W as well as another one upstream the Antarctic Peninsula.

Each panel of Fig. 10, representing one method, shows the deviation of strong moisture flux of these method with respect to the method mean (note the different color bar for the method mean and the deviations). Comparison reveals differing behaviors. There are methods which over- and underestimate the maximum at Prime meridian (M06, M10, M18) others show variations around East Antarctica between 30°E and 90°E. However, the deviation from method mean has generally a small proportion for *WED* and *EA*. It is noticeable that there are considerable larger differences between the methods in the ABS region. Here, the calculation of moisture flux anomalies is also sensitive to the width of the longitudinal sector used for the attribution of moisture transport to strong cyclones (not shown). In the other regions around the Antarctic continent, mainly the intensity but not location and sign of moisture flux anomaly is sensitive to the width of the sector.

4. Discussion

Our analysis has considered many aspects of subantarctic cyclone behavior and, as far as they can be compared, our results are consistent with the earlier findings of Neu et al. (2013). The various methods differ in the number of cyclones identified. Also the track-to-track comparison in the region of the SO does not show a systematically different result in comparison to the analysis of the entire SH (Neu et al. 2013).

The 14 cyclone identification and tracking methods analyzed in this study use different input variables which lead to a grouping according to vorticity-based and MSLP/geopotential

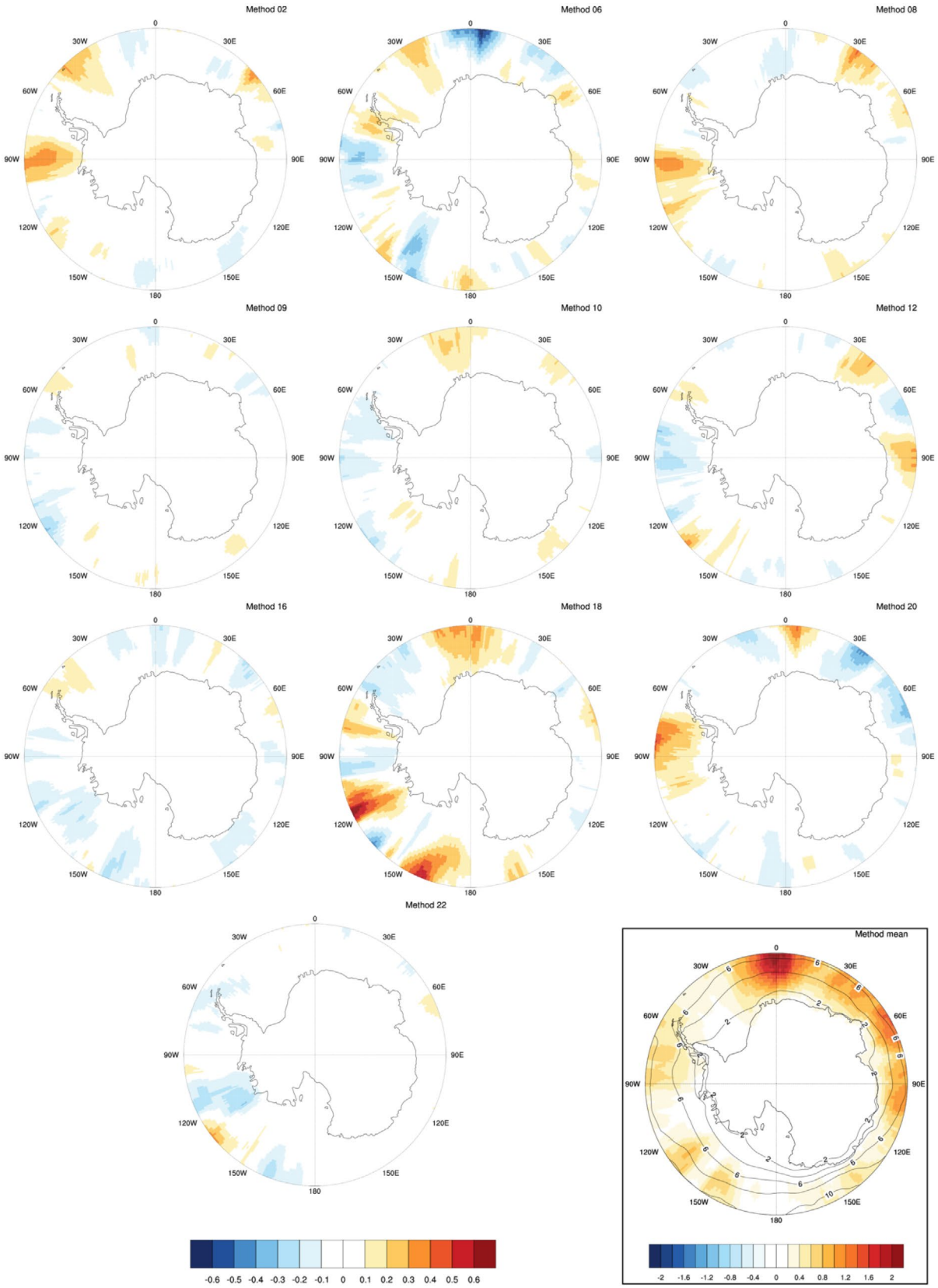

Fig. 10. Composite of transient meridional moisture flux anomaly [$kgm^{-1}s^{-1}$] for all days where the maximum intensity of strong winter (JJA) cyclones is identified (bottom box) for the method mean. Moisture flux is calculated in a 60° longitudinal sector around cyclone center. Flux anomalies (color shadings) are calculated with respect to the long term (1979–2008) mean for JJA (contour lines). Each method panel shows the flux deviation w.r.t. to the method mean. Note the different color bar for the method mean and the deviations of the mean. Poleward moisture flux is defined to be positive.

height-based methods. Vorticity better reflects the synoptic high frequency scale, whereas MSLP is better at the low-frequency scale (Hodges et al. 2003). Vorticity-based methods are able to identify cyclones in an earlier stage of their lifecycle even without finding a closed isobar. However, moving vorticity maxima are not always associated with pressure minima (Neu et al. 2013).

One of the peculiarities of the Antarctic environment is steep topography, which can influence cyclone tracking methods, e.g., to identify spurious lows (Simmonds et al., 1999b). Regional orography potentially is the reason for the difference in identifying the absolute maximum of system density which is located on the ice shelf regions by 6 of the 14 methods (M02, M07, M14, M16, M20, and M21). Furthermore, M07 identifies extraordinary pronounced maxima over the Ronne, Ross and Amery Ice Shelves. Cyclone identification methods typically make use of pre-processing of input variables, e.g. smoothing, and/or post-processing steps of identified lows or tracks, e.g. filtering lows of certain strength or tracks of certain lifetime and travelling distance. These steps are generally part of the identification methods to deal with spurious lows. The sensitivity of the pre- and post-processing is typically found empirically by means of the identification of known climatologies as well as case studies. The steep orography and strong local winds in the areas around the large ice shelves seem to be sensitive regions for the identification methods. Since these differences of the methods are potentially due to local effects, it may be possible to homogenize the results with consistent post-processed filtering of tracks with respect to their travelling distance. In a multi-method study, it is hardly possible to argue about the truth. In the end, case studies would be necessary to learn more about the sensitivity of each single method, especially in the regions of disagreement.

With respect to the number of identified cyclone tracks, the spread between methods is more pronounced in winter than summer. This might be due to small depressions which add noise to the frequency and the different sensitivity of the methods to these small systems. A trend analysis of cyclone frequency shows significant trends for *S60* in DJF possibly due to the positive summer trend of SAM during the twentieth century (Hartmann et al., 2013; Simmonds, 2015) illustrating a link between cyclone frequency and SAM for summer identified consistently for all methods. However, this connection is not robust in winter among the methods. Pezza et al. (2008) found a link between winter SAM and cyclone frequency, location and intensity. They used the method of Murray and Simmonds (1991a) which also shows a distinct connection with SAM in our study (M10). For JJA, five methods (M02, M06, M10, M15, M18) demonstrate robust links between SAM and the number of tracks in three or even in all four regions, while five other methods (M09, M16, M20, M21, M22) show that in all regions the correlation fails to achieve statistical significance (at 5% level). Three methods which show the robust link to SAM are vorticity based (M02, M10, M18) and M06 is a hybrid one, whereas M15 uses geopotential height as input variable. Vorticity-based methods tend to identify cyclone centers poleward compared to MSLP/geopotential height-based methods. Pezza et al. (2008) used a correlation map on the SO, which shows a shift of the location of cyclone tracks depending on the SAM phase. Our study correlates the number of cyclone tracks in *S60* and the three sectors, respectively, with SAM. There could potentially be sensitivities of the choice of the region (south of 60°S in our study) and the value of the correlation. The correlation of cyclone frequency and an index representing the strength of the ABSL seems to show more pronounced values for the vorticity based methods. These methods possibly have an advantage to identify tracks in region of the ABSL where deep pressure background fields can be found.

Transient waves have a strong impact on SH poleward moisture transport and thus influencing Antarctic mass balance. Extra-tropical cyclones are the main contributor to the TE component of moisture flux (Peixoto and Oort, 1992), whereas intense cyclones play a major role. The main part of poleward transport is found in winter (Cullather et al., 1998). The analysis of the relationship between strong cyclones and transient moisture flux is an impact study of extra-tropical depression in the SO. Clearly, the regions of increased moisture flux are related to the occurrence of strong cyclone activity. Overall, there are three major regions of moisture inflow into Antarctica, i.e. the region of Dronning Maud Land, Wilkes Land and Marie Byrd Land (Cullather et al., 1998). The evaluation of the attribution of transient moisture flux to strong cyclones shows the importance of these severe synoptic systems for Antarctic moisture transport, at least at Dronning Maud Land and Wilkes Land, and this relation is robustly identified by all methods. Although, there are many strong cyclones identified in the *ABS* region, moisture flux anomaly due to these depressions is small. This is possibly due to the ABSL which significantly contributes to the TE component of the moisture flux independently of cyclone activity (Grieger et al., 2016). Main differences between the methods can be found in the *ABS* sector. Attribution of moisture transport to strong depressions seems to be difficult in this region where cyclones are embedded in a deep MSLP background field.

5. Summary and conclusion

This study presents a comprehensive analysis of winter and summer subantarctic cyclones and their characteristics, as identified by 14 objective identification and tracking algorithms for extra-tropical cyclones based on the ERA-Interim reanalysis. Four regions are investigated in detail as mechanisms and modes of variability may have a different spatial imprint. It has been shown in previous studies (e.g., Neu et

al., 2013), that the number of identified cyclones varies for the different methods, and we find this to be also true for subantarctic synoptic features. Interestingly, the spread of identified cyclone track numbers between the methods is larger in winter than in summer, where cyclones are generally less intense. This is explained by the smaller range of cyclone intensity. The horizontal patterns of cyclone track densities vary for the different methods. Although most algorithms agree in identifying major local maxima, single methods show distinct outliers, e.g. over the Amery Ice Shelf or the Antarctic Peninsula. As expected, the horizontal patterns are more similar for the strongest cyclones.

The findings of our trend analysis differ with region and season. Significant positive trends in track numbers are found for DJF for the entire subantarctic region (*S60*) and *ABS*. Here, 12 of 14 methods show significant positive trends. For winter, also most methods show positive trends, whereas only for half of the methods these trends are significant. For the three regions around Antarctica there are even fewer methods showing this positive trend. The trend analysis further shows that the statistical significance and, to a lesser extent the sign, of the trend depends on the method used, which calls for caution when only one cyclone detection and tracking method is at hand (in agreement with what Raible et al. [2008] found for the North Atlantic).

A relationship between winter cyclone frequency and large-scale drivers is also not consistently apparent for the regions analyzed. On the other hand, in summer when trends of the large-scale drivers such as SAM are more pronounced (Hartmann et al., 2013), the association with cyclone frequency is quite robust especially for the entire region surrounding Antarctica. Our analysis highlights the impact of strong cyclone activity on poleward moisture transport and shows the robustness of the link between the most intense cyclone tracks and its related moisture flux. This result shows the consistent representation of physical processes independently of the tracking method used. The nature of a cyclones allows for different definitions of these complex features. Each method uses different thresholds of pre- or post-processing procedures to define a track or reject spurious lows, which are typically of low intensity. Therefore, results better agree for the strongest cyclone tracks. With respect to the numerous characteristics of cyclones, this study finally shows the benefit of using multi-methods (or an 'ensemble' of methods) to better estimate robustness and uncertainties.

Disclosure statement

No potential conflict of interest was reported by the authors.

Funding

This work was supported by the Australian Research Council [grant number DP16010997]; Antarctic Science Advisory Committee [grant number 4080]; German Federal Ministry for Education and Research through the research program MiKlip (FKZ: 01LP1520A); EU Marie Curie CI Grant EVE [grant number 322208]; Schweizerischer Nationalfonds zur Förderung der Wissenschaftlichen Forschung [grant number 200020_172745] and by courtesy of the contract #14.613.21.0083 (ID RFMEFI61317X0083) with the Ministry of Education and Science of Russian Federation.

References

Akperov, M. G., Bardin, M. Y., Volodin, E. M., Golitsyn, G. S. and Mokhov, I. I. 2007. Probability distributions for cyclones and anticyclones from the NCEP/NCAR reanalysis data and the INM RAS climate model. *Izvest. Atmos. Ocean. Phys.* **43**, 705–712. DOI:10.1134/s0001433807060047.

Bardin, M. Y. and Polonsky, A. B. 2005. North Atlantic Oscillation and synoptic variability in the European-Atlantic region in winter. *Izvest. Atmos. Ocean. Phys.* **41**, 127–136.

Blender, R., Fraedrich, K. and Lunkeit, F. 1997. Identification of cyclone-track regimes in the North Atlantic. *Quart. J. R. Meteor. Soc.* **123**, 727–741.

Blender, R. and Schubert, M. 2000. Cyclone tracking in different spatial and temporal resolutions. *Mon. Wea. Rev.* **128**, 377–384.

Bracegirdle, T. J. and Marshall, G. J. 2012. The reliability of Antarctic tropospheric pressure and temperature in the latest global reanalyses. *J. Climate* **25**, 7138–7146. DOI:10.1175/JCLI-D-11-00685.1.

Bromwich, D. H., Robasky, F. M., Cullather, R. I. and Van Woert, M. L. 1995. Atmospheric hydrologic cycle over the Southern Ocean and Antarctica from operational numerical analyses. *Mon. Wea. Rev.* **123**, 3518–3538.

Cullather, R. I., Bromwich, D. H. and Van Woert, M. L. 1998. Spatial and temporal variability of Antarctic precipitation from atmospheric methods. *J. Clim.* **11**, 334–367.

Dee, D. P., Uppala, S. M., Simmons, A. J., Berrisford, P., Poli, P. and co-authors. 2011. The ERA-interim reanalysis: Configuration and performance of the data assimilation system. *Quart. J. R. Meteor. Soc.* **137**, 553–597. DOI:10.1002/qj.828.

Flaounas, E., Kotroni, V., Lagouvardos, K. and Flaounas, I. 2014. CycloTRACK (v1.0) – tracking winter extratropical cyclones based on relative vorticity: Sensitivity to data filtering and other relevant parameters. *Geosci. Model Dev.* **7**, 1841–1853. DOI:10.5194/gmd-7-1841-2014.

Fogt, R. L., Wovrosh, A. J., Langen, R. A. and Simmonds, I. 2012. The characteristic variability and connection to the underlying synoptic activity of the Amundsen–Bellingshausen Seas Low. *J. Geophys. Res.* **117**, D07111. DOI:10.1029/2011JD017337.

Fyfe, J. C. 2003. Extratropical Southern Hemisphere cyclones: Harbingers of climate change? *J. Clim.* **16**(17), 2802–2805.

Gong, D. and Wang, S. 1999. Definition of Antarctic Oscillation index. *Geophys. Res. Lett.* **26**, 459–462.

Grieger, J., Leckebusch, G. C., Donat, M. G., Schuster, M. and Ulbrich, U. 2014. Southern Hemisphere winter cyclone activity under recent and future climate conditions in multi-model AOGCM simulations. *Int. J. Climatol.* **34**, 3400–3416. DOI:10.1002/joc.3917.

Grieger, J., Leckebusch, G. C. and Ulbrich, U. 2016. Net precipitation of Antarctica: Thermodynamical and dynamical parts of the climate change signal. *J. Clim.* **29**(3), 907–924.

Hartmann, D., Klein Tank, A. M. G., Rusticucci, M., Alexander, L.V., Brönnimann, S. and co-authors. 2013. Observations: Atmosphere and surface. In: *Climate Change 2013: The Physical Science Basis. Contribution of Working Group I to the Fifth Assessment Report of the Intergovernmental Panel on Climate Change* (eds. T. F. Stocker, D. Qin, G.-K. Plattner, M. Tignor and S. K. Allen and co-authors). Cambridge Univ. Press, Cambridge.

Hewson, T. D. and Titley, H. A. 2010. Objective identification, typing and tracking of the complete life-cycles of cyclonic features at high spatial resolution. *Meteor. Appl.* **17**, 355–381. DOI:10.1002/met.204.

Hodges, K. I., Hoskins, B. J., Boyle, J. and Thorncroft, C. 2003. A comparison of recent reanalysis datasets using objective feature tracking: Storm tracks and tropical easterly waves. *Mon. Wea. Rev.* **131**, 2012–2037.

Hosking, J. S., Orr, A., Marshall, G. J., Turner, J. and Phillips, T. 2013. The influence of the Amundsen–Bellingshausen Seas Low on the climate of West Antarctica and its representation in coupled climate model simulations. *J. Clim.* **26**(17), 6633–6648.

Hoskins, B. J. and Hodges, K. I. 2005. A new perspective on southern hemisphere storm tracks. *J. Clim.* **18**, 4108–4129. DOI:10.1175/JCLI3570.1.

Inatsu, M. 2009. The neighbor enclosed area tracking algorithm for extratropical wintertime cyclones. *Atmos. Sci. Lett.* **10**, 267–272.

Kew, S. F., Sprenger, M. and Davies, H. C. 2010. Potential vorticity anomalies of the lowermost stratosphere: A 10-yr winter climatology. *Mon. Wea. Rev.* **138**, 1234–1249. DOI:10.1175/2009MWR3193.1.

Lambert, S. J. and Fyfe, J. C. 2006. Changes in winter cyclone frequencies and strengths simulated in enhanced greenhouse warming experiments: results from the models participating in the IPCC diagnostic exercise. *Climate Dyn.* **26**, 713–728.

Leckebusch, G. C., Donat, M., Ulbrich, U. and Pinto, J. G. 2008. Mid-latitude cyclones and storms in an ensemble of European AOGCMs under ACC. *CLIVAR Exch.* **13**, 3–5.

Leckebusch, G. C., Koffi, B., Ulbrich, U., Pinto, J. G., Spangehl, T. and co-authors. 2006. Analysis of frequency and intensity of European winter storm events from a multi-model perspective, at synoptic and regional scales. *Clim. Res.* **31**, 59–74.

Leckebusch, G. C. and Ulbrich, U. 2004. On the relationship between cyclones and extreme windstorm events over Europe under climate change. *Global Planet. Change* **44**, 181–193.

Lionello, P., Dalan, F. and Elvini, E. 2002. Cyclones in the Mediterranean region: The present and the doubled CO_2 climate scenarios. *Clim. Res.* **22**, 147–159.

Meneghini, B., Simmonds, I. and Smith, I. N. 2007. Association between Australian rainfall and the Southern Annular Mode. *Int. J. Climatol.* **27**, 109–121.

Murphy, B. F. and Simmonds, I. 1993. An analysis of strong wind events simulated in a GCM near Casey in the Antarctic. *Mon. Wea. Rev.* **121**, 522–534.

Murray, R. J. and Simmonds, I. 1991a. A numerical scheme for tracking cyclone centres from digital data. Part I: Development and operation of the scheme. *Aust. Meteor. Mag.* **39**, 155–166.

Murray, R. J. and Simmonds, I. 1991b. A numerical scheme for tracking cyclone centres from digital data. Part II: Application to January and July GCM simulations. *Aust. Meteor. Mag.* **39**, 167–180.

Neu, U., Akperov, M. G., Bellenbaum, N., Benestad, R., Blender, R. and co-authors. 2013. IMILAST: A community effort to intercompare extratropical cyclone detection and tracking algorithms. *Bull. Amer. Meteor. Soc.* **94**, 529–547. DOI:10.1175/BAMS-D-11-00154.1.

Peixoto, J. P. and Oort, A. H. 1992. *Physics of Climate*. American Institute of Physics, New York, 520 pp.

Pezza, A. B., Durrant, T., Simmonds, I. and Smith, I. 2008. Southern Hemisphere synoptic behavior in extreme phases of SAM, ENSO, sea ice extent, and southern Australia rainfall. *J. Clim.* **21**, 5566–5584.

Pezza, A. B., Rashid, H. and Simmonds, I. 2012. Climate links and recent extremes in Antarctic sea ice, high-latitude cyclones, Southern Annular Mode and ENSO. *Clim. Dyn.* **38**, 57–73. DOI:10.1007/s00382-011-1044-y.

Pezza, A. B., Simmonds, I. and Renwick, J. A. 2007. Southern hemisphere cyclones and anticyclones: Recent trends and links with decadal variability in the Pacific Ocean. *Int. J. Climatol.* **27**, 1403–1419. DOI:10.1002/joc.1477.

Pinto, J. G., Spangehl, T., Ulbrich, U. and Speth, P. 2005. Sensitivities of a cyclone detection and tracking algorithm: Individual tracks and climatology. *Meteor. Z.* **14**, 823–838.

Raible, C. C., Della-Marta, P. M., Schwierz, C., Wernli, H. and Blender, R. 2008. Northern Hemisphere extratropical cyclones: A comparison of detection and tracking methods and different reanalyses. *Mon. Wea. Rev.* **136**, 880–897.

Raphael, M. N., Marshall, G. J., Turner, J., Fogt, R., Schneider, D. and co-authors. 2016. The Amundsen Sea Low: variability, change, and impact on Antarctic climate. *Bull. Amer. Meteor. Soc.* **97**, 111–121. DOI:10.1175/bams-d-14-00018.1.

Rudeva, I. and Gulev, S. K. 2007. Climatology of cyclone size characteristics and their changes during the cyclone life cycle. *Mon. Wea. Rev.* **135**, 2568–2587.

Rudeva, I., Gulev, S. K., Simmonds, I. and Tilinina, N. 2014. The sensitivity of characteristics of cyclone activity to identification procedures in tracking algorithms. *Tellus* **66A**, 24961. DOI:10.3402/tellusa.v66.24961.

Rudeva, I. and Simmonds, I. 2015. Variability and trends of global atmospheric frontal activity and links with large-scale modes of variability. *J. Clim.* **28**, 3311–3330. DOI:10.1175/JCLI-D-14-00458.1.

Schwerdtfeger, W., 1984: *Weather and Climate of the Antarctic*. Elsevier, Amsterdam, New York, 261 pp.

Serreze, M. C. 1995. Climatological aspects of cyclone development and decay in the Arctic. *Atmos. Ocean* 33, 1–23.

Simmonds, I. 2000. Size changes over the life of sea level cyclones in the NCEP reanalysis. *Mon. Wea. Rev.* **128**, 4118–4125.

Simmonds, I. 2015. Comparing and contrasting the behaviour of Arctic and Antarctic sea ice over the 35-year period 1979–2013. *Ann. Glaciol.* **56**(69), 18–28. DOI:10.3189/2015AoG69A909.

Simmonds, I., Bi, D. and Hope, P. 1999a. Atmospheric water vapor flux and its association with rainfall over China in summer. *J. Clim.* **12**, 1353–1367.

Simmonds, I., Burke, C. and Keay, K. 2008. Arctic climate change as manifest in cyclone behavior. *J. Clim.* **21**, 5777–5796.

Simmonds, I. and Keay, K. 2000. Mean Southern Hemisphere extratropical cyclone behavior in the 40-year NCEP–NCAR reanalysis. *J. Clim.* **13**, 873–885.

Simmonds, I., Keay, K. and Lim, E.-P. 2003. Synoptic activity in the seas around Antarctica. *Mon. Wea. Rev.* **131**, 272–288.

Simmonds, I. and King, J. C. 2004. Global and hemispheric climate variations affecting the Southern Ocean. *Antarc. Sci.* **16**, 401–413. DOI:10.1017/S0954102004002226.

Simmonds, I. and Lim, E.-P. 2009. Biases in the calculation of Southern Hemisphere mean baroclinic eddy growth rate. *Geophys. Res. Lett.* **36**, L01707. DOI:10.1029/2008GL036320.

Simmonds, I., Murray, R. J. and Leighton, R. M. 1999b. A refinement of cyclone tracking methods with data from FROST. *Australian Meteorological Magazine* (SI), 35–49.

Simmonds, I. and Wu, X. 1993. Cyclone behaviour response to changes in winter southern hemisphere sea-ice concentration. *Quart. J. R. Meteor. Soc.* **119**, 1121–1148.

Sinclair, M. R. 1994. An objective cyclone climatology for the Southern Hemisphere. *Mon. Wea. Rev.* **122**, 2239–2256.

Sinclair, M. R. 1997. Objective identification of cyclones and their circulation intensity, and climatology. *Wea. Forecasting* **12**, 595–612.

Trigo, I. F. 2006. Climatology and interannual variability of storm-tracks in the Euro-Atlantic sector: a comparison between ERA-40 and NCEP/NCAR reanalyses. *Clim. Dyn.* **26**, 127–143.

Turner, J., Bindschadler, R., Convey, P., di Prisco, G., Fahrbach, E., Gutt, J., Hodgson, D. P. M. and Summerhayes, C. (eds.) 2009. *Antarctic climate change and the environment* Scientific Committee on Antarctic Research, Scott Polar Research Institute, Cambridge.

Turner, J., Bromwich, D., Colwell, S., Dixon, S., Gibson, T. and co-authors. 1996. The Antarctic First Regional Observing Study of the Troposphere (FROST) project. *Bull. Amer. Meteor. Soc.* **77**, 2007–2032. DOI:10.1175/1520-0477(1996)077<2007:TAFROS>2.0.CO;2.

Turner, J., Phillips, T., Hosking, J. S., Marshall, G. J. and Orr, A. 2013. The Amundsen Sea low. *Int. J. Climatol.* **33**(7), 1818–1829.

Ulbrich, U., Leckebusch, G. C., Grieger, J., Schuster, M., Akperov, M. and co-authors 2013. Are greenhouse gas signals of Northern Hemisphere winter extra-tropical cyclone activity dependent on the identification and tracking algorithm? *Meteor. Z.* **22**, 61–68. DOI:10.1127/0941-2948/2013/0420.

Uotila, P., Vihma, T., Pezza, A. B., Simmonds, I., Keay, K. and co-authors. 2011. Relationships between Antarctic cyclones and surface conditions as derived from high resolution NWP data. *J. Geophys. Res.* **116**, D07109. DOI:10.1029/2010JD015358.

Wang, X. L., Swail, V. R. and Zwiers, F. W. 2006. Climatology and changes of extratropical cyclone activity: Comparison of ERA-40 with NCEP–NCAR reanalysis for 1958–2001. *J. Clim.* **19**, 3145–3166.

Wernli, H. and Schwierz, C. 2006. Surface cyclones in the ERA-40 dataset (1958–2001). Part I: Novel identification method and global climatology. *J. Atmos. Sci.* **63**, 2486–2507.

Zolina, O. and Gulev, S. K. 2002. Improving the accuracy of mapping cyclone numbers and frequencies. *Mon. Wea. Rev.* **130**, 748–759.